# River Flow 2004

**Chapter** · January 2004

CITATIONS
0

READS
284

**2 authors:**

Mouldi Ben Meftah
Polytechnic University of Bari
**126** PUBLICATIONS **1,023** CITATIONS
SEE PROFILE

Michele Mossa
Polytechnic University of Bari
**395** PUBLICATIONS **3,573** CITATIONS
SEE PROFILE

# Experimental study of the scour hole downstream of bed sills

M. Ben Meftah
*Water Engineering and Chemistry Department, Technical University of Bari, Italy*

M. Mossa
*Civil and Environmental Engineering Department, Technical University of Bari, Italy*

ABSTRACT: An experimental study on long local scouring downstream of bed sills in monogranular sand bed was carried out in the hydraulic laboratory flume at the Mediterranean Agronomic Institute of Bari (Italy). The main objectives of this study are the determination of the scour hole dimensions, with its maximum scour depth, at the equilibrium stage, and the investigation of the influence of sills on the distribution of the three velocity components through the scour hole at the same stage. Four experimental configurations were tested, the main difference between them being the distance between sills. Based on experimental data, the classical dimensional analysis of the variables that influence the development of the scour hole has been carried out in order to obtain two empirical formulas predicting the maximum scour depth and the length of the scour hole at the equilibrium stage. Moreover, it was observed that the distance between sills influences the scour hole dimension and shape. The three velocity components of the flow, measured with an Acoustic Doppler Velocimeter (ADV), show that in the scour hole, at the equilibrium stage, the three-components of the flow turbulence intensities are very high. Near-bed flow vortexes in addition to secondary currents are also observed.

## 1 INTRODUCTION

The bed in the direct neighborhood of hydraulic structures is generally protected against current and eddies. The length of the bed protection depends on the permissible scour (maximum scour depth and upstream scour slope). When the length of the bed protection is increased, the scour process is less intense due to the decay of turbulence energy and the adaptation of the velocity profile downstream of the hydraulic structure. For a designer, the most important scour parameter is the maximum scour depth in the equilibrium phase, defined as the time when the scour hole and the bed profile spatial characteristics along the flume do not change any longer. Anyway, the extent of the scour hole is strongly dependent on time. Initially, the scour development with time is rapid, then it decreases gradually to reach the equilibrium stage after a long time. The magnitude of the maximum scour depth depends on the bed shear stress, the turbulence condition near the bed, the sediment characteristic (density of the bed material, sediment-size distribution, porosity, cohesive or non-cohesive bed material, etc.).

In gravel bed rivers, bed sills are used to limit bed degradation and to control erosion in the proximity of bridge piers or in channels downstream of stilling basins of dams. There is extensive literature on scour (Borman, 1988; Breusers, 1966; Habib et Al., 1994 ; Hoffmans et Al., 1995 ; Hoffmans and Verheig, 1997; Hoffmans, 1998; Javal and Kenneth, 1985; Kandasany and Melville, 1998; Smith and Strang, 1967; Van der Meulen and Vinje, 1995).

In addition, the bed sill could have a number of impacts upon the flow velocity, and the impacts from the sill can vary spatially. Furthermore, the presence of the bed sill causes a redistribution of the flow velocity. It can decrease or increase the flow turbulence, create vortex phenomenon and/or secondary current velocity.

This study is concerned with an experimental investigation of the scour hole phenomenon due to a current flowing over sills in an erodible bed of sand particles. The variation of the scour hole with time, the equilibrium water and bed profiles, in addition to the three flow velocity components at different sections along the channel were assessed for each configuration. Two different scour hole topologies were observed, depending upon the distance between sills.

## 2 THEORETICAL BACKGROUND

Local scour hole is typical of non-cohesive bed river, downstream of the bed sills. After a long period of time the scour hole reaches an equilibrium state. At the equilibrium, the geometry of the system under

consideration is shown in Figure 1 (Gaudio et Al., 2000).

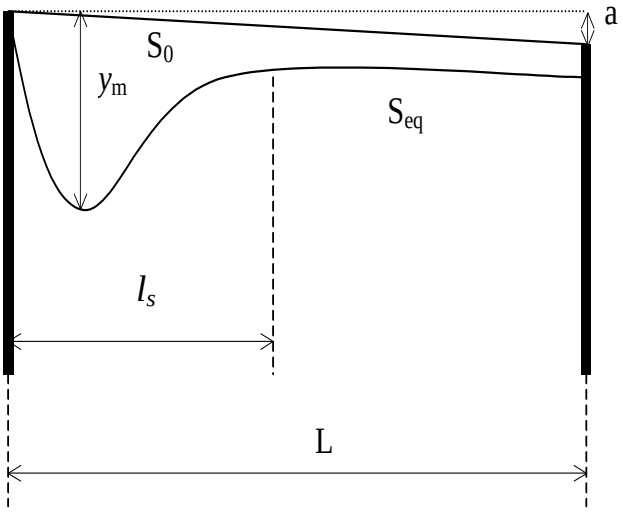


Figure 1. Sketch of the scour hole

Based on this geometric shape of the bed profile, the maximum scour depth $y_m$, or the scour length $l_s$, can be expressed as:

$$y_m \text{ or } l_s = f(g, \nu, \rho_w, \rho_s, q, h_u, d_{50}, L, a) \quad (1)$$

where g is the gravity acceleration, ν = kinematic water viscosity, $\rho_w$ = water density, $\rho_s$ = sediment density, q = discharge per unit width, $h_u$ = flow depth over the sill, $d_{50}$ = grain size for which 50% of the total weight of the sediment is finer, L = distance between sills, and a = difference between the level of two successive sills, a is calculated as:

$$a = L \cdot S_0 \quad (2)$$

where $S_0$ is the initial bed slope.

The application of the *Buckingham Π theorem* to equations (1) leads to:

$$\frac{y_m}{h_u} \text{ or } \frac{l_s}{h_u} = f\left(\frac{q^2}{g h_u^3 \Delta}, \frac{q}{\nu}, \frac{\Delta d_{50}}{h_u}, \frac{L}{h_u}, \frac{\Delta a}{h_u}\right) \quad (3)$$

where:

$$\Delta = \frac{\rho_s - \rho_w}{\rho_w}. \quad (4)$$

The $q^2/gh_u^3\Delta$ ratio is the square of the Froude number Fr, and the $q/\nu$ ratio is the Reynolds number. Generally, in open-channels, the flow is almost always fully turbulent. Thus, the dependence upon the Reynolds number could be neglected. Since the parameter *a* is determined as the product of the distance between sills L and the initial bed slope $S_0$, the ratio $L/h_u$ can be removed from equations (3). Furthermore, the effect of the channel width is here implicitly neglected by choosing variables per unit width. In addition, in the present study sand grains have an almost constant value of the relative submerged particle density, Δ, equal to about 1.65. Because of this constancy, the effect of Δ is not shown in the present study.

According to these simplifying assumptions, equations (3) can be reduced to:

$$\frac{y_m}{h_u} \text{ or } \frac{l_s}{h_u} = f\left(\frac{q^2}{g h_u^3 \Delta}, \frac{\Delta d_{50}}{h_u}, \frac{\Delta L S_0}{h_u}\right) \quad (5)$$

The determination of equations (5) was one of the main objectives of the present paper.

## 3 EXPERIMENTAL SET-UP

The experimental work was carried out in a horizontal flume in the laboratory of the Mediterranean Agronomic Institute of Bari (Italy). This flume is 7.72 m long, 0.30 m wide, and has a depth of 0.40 m. The floor of the flume is constructed with Plexiglas, while the lateral walls are made of glass, which allows us better side viewing of the flow. Water is fed in from an upstream reservoir with a maximum charge of 54 cm equipped with stilling grid and lateral weir, which maintains a constant head upstream of a movable gate constructed at the upstream end of the flume. This gate is made of Plexiglas and allows the passage of different discharges with different corresponding channel flow depths. The flume is supplied by a pump with maximum discharge of 24 l/s through a steel pipe. To create a smooth flow transition from the upstream reservoir to the flume, a wooden ramp was placed at the inlet of the flume; the wooden ramp is 1.55 m long, 0.15 m thick and has the same width of the channel cross section (Figure 2).

At the downstream end of the flume, water is intercepted by a stilling reservoir, equipped with three vertical grids to stabilize water, and a triangular weir (V-notch sharp crested weir) to measure the flow discharge.

To protect against erosion of the sand bed of the flume, control sills were placed along the channel. Four sets of tests were performed during the experimental work, the difference between them being the distance (L) between sills (Set 1: L = 1 m; Set 2: L = 2 m; Set 3: L = 4 m; Set 4: L = 3 m). The sill level decreases progressively going from the upstream section to the downstream section of the channel, respecting a constant initial slope fixed at the value of 0.0086. The sills used in the experiments consisted of PVC plates 0.30 m wide and 0.01 m thick (Figure 1).

The flume bottom is covered with an erodible bed material layer consisting of sand particles with mean average size ($d_{50}$) of 1.8 mm and specific density of 2.65 g/cm$^3$. The grain-size distribution curve of the sand is illustrated in Figure 3. The uniformity coefficient $C_u = d_{60}/d_{10}$ was equal to 1.6, where $d_{60}$ = grain size for which 60% of the total weight of the sediment is finer and $d_{10}$ = grain size for which 10% of the total weight of the sediment is finer. Thus, the sediment can be considered as uniform. Along the

channel, the sand layer decreases progressively from the upstream sections to the downstream sections, respecting the initial slope predetermined by the sills.

During the experiments, the bed profile along the channel at various times was marked on the glass side-walls of the flume by means of different colors. At the equilibrium stage, the water level profile along the centerline was measured using an electrical hydrometer with an accuracy of 1/10 of millimeter. At the same stage, the bed profiles along the centerline and near the two side-walls of the channel were determined using a point gage with an accuracy of 1/10 of millimeter.

In order to study the effects of the sill upon the flow velocity at the equilibrium, the measurements of the three-velocity components along the flume at different positions have been recorded during this experimental work, using an Acoustic- Doppler Velocimeter (ADV).

Figure 2. Laboratory flume

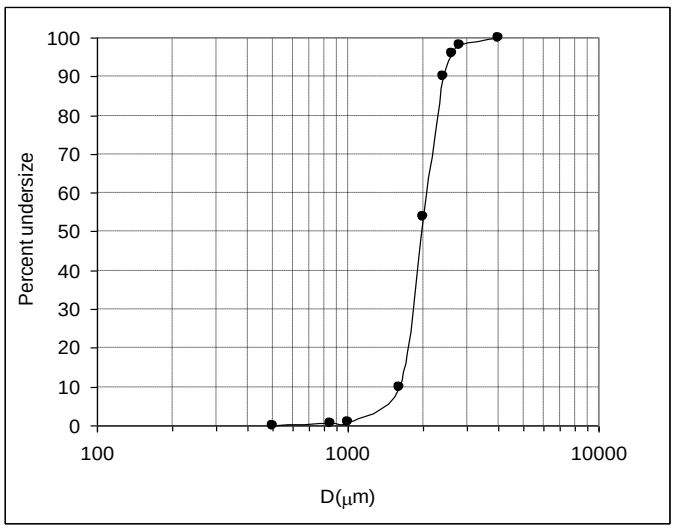


Figure 3. Grain-size distribution curve

The main parameters of the tests are illustrated in Table 1, where, Q = flow discharge through the channel, T = water temperature, and $t_d$ = total duration of each test.

Table 1. Main parameters of each test

| No. | Test | Q ($m^3/s$) | q ($m^2/s$) | L (m) | $t_d$ (h) | T (°C) |
|---|---|---|---|---|---|---|
| 1 | T04 | 0.006 | 0.021 | 1 | 25 | 13 |
| 2 | T05 | 0.010 | 0.033 | 1 | 29 | 15 |
| 3 | T06 | 0.005 | 0.015 | 1 | 25 | 15 |
| 4 | T07 | 0.012 | 0.039 | 1 | 26 | 16 |
| 5 | T08 | 0.008 | 0.027 | 1 | 27 | 19 |
| 6 | T09 | 0.006 | 0.021 | 2 | 27 | 19 |
| 7 | T10 | 0.006 | 0.027 | 2 | 24 | 20 |
| 8 | T11 | 0.010 | 0.033 | 2 | 27 | 21 |
| 9 | T12 | 0.012 | 0.044 | 2 | 27 | 22 |
| 10 | T13 | 0.014 | 0.046 | 2 | 26 | 23 |
| 11 | T14 | 0.006 | 0.020 | 4 | 25 | 25 |
| 12 | T15 | 0.008 | 0.027 | 4 | 25 | 25 |
| 13 | T16 | 0.010 | 0.033 | 4 | 25 | 26 |
| 14 | T17 | 0.005 | 0.016 | 4 | 25 | 27 |
| 15 | T18 | 0.005 | 0.015 | 3 | 25 | 27 |
| 16 | T19 | 0.006 | 0.021 | 3 | 25 | 27 |
| 17 | T20 | 0.008 | 0.027 | 3 | 25 | 27 |
| 18 | T21 | 0.010 | 0.033 | 3 | 25 | 27 |
| 19 | T22 | 0.012 | 0.040 | 3 | 25 | 27 |

Table 2. Measured variables

| No. | Test | $y_m$ (m) | $h_u$ (m) | $l_s$ (m) |
|---|---|---|---|---|
| 1 | T04 | 0.039 | 0.03 | (*) |
| 2 | T05 | 0.088 | 0.054 | (*) |
| 3 | T06 | 0.028 | 0.026 | (*) |
| 4 | T07 | 0.105 | 0.062 | (*) |
| 5 | T08 | 0.064 | 0.043 | (*) |
| 6 | T09 | 0.053 | 0.035 | 1.2 |
| 7 | T10 | 0.057 | 0.042 | 1.3 |
| 8 | T11 | 0.070 | 0.054 | 1.6 |
| 9 | T12 | 0.081 | 0.063 | 1.8 |
| 10 | T13 | 0.090 | 0.070 | 2.0 |
| 11 | T14 | 0.076 | 0.032 | 1.4 |
| 12 | T15 | 0.090 | 0.043 | 1.7 |
| 13 | T16 | 0.112 | 0.054 | 2.1 |
| 14 | T17 | 0.065 | 0.027 | 1.1 |
| 15 | T18 | 0.050 | 0.027 | 1.0 |
| 16 | T19 | 0.061 | 0.035 | 1.2 |
| 17 | T20 | 0.071 | 0.043 | 1.4 |
| 18 | T21 | 0.084 | 0.052 | 1.7 |
| 19 | T22 | 0.094 | 0.062 | 2.0 |

(*)Quasi-parabolic shape of the scour hole (see below)

During all the experimental work, the measurement of the flow depth over sills, $h_u$, the maximum scour depth, $y_m$, and the length of the scour hole, $l_s$, were assessed for each test. The flow depth over a sill was measured as the vertical distance between the top of the sill and the water profile. The maximum scour depth was determined as the vertical distance between the initial bed profile and the center of the scour hole at the equilibrium stage. The scour length was determined as the distance between the

sill and the point downstream of the scour hole where the slope reaches a constant value. The aforementioned variables are shown in Table 2. For tests T04 to T08, the scour hole occupied all of the space between the sills, and, therefore, $l_s$ was not determined.

## 4 RESULTS

### 4.1 *Scour hole progress*

Examining all the tests, it has been shown that the extent of the scour hole is strongly dependent on time. So, it was observed that there are three stages of the local scour hole development.

Initially, the scour hole development with time is rapid, and this is due to the high rate of solid transport achieved on the downstream end of each sill. The high rate of the solid transport is a consequence of the high forces of the bed-shear stresses exerted over the sand bed at the initial time. To study the different stages of the development of the scour hole as a function of the time for each test, and their similarity, the values of $y_t/y_m$ have been plotted against $t/t_d$ (where $y_t$ is the scour hole depth at time t, and $t_d$, as written, is the duration of each experiment, i.e. the time when the scour hole reached the equilibrium phase). Figure 4 shows that the scour development as a function of time presents three different phases. Figure 4 shows, as well, that at the initial stage the scour hole depth for each test reaches about 65% of the maximum scour depth during a time less than 10% of the duration after which the equilibrium stage was reached.

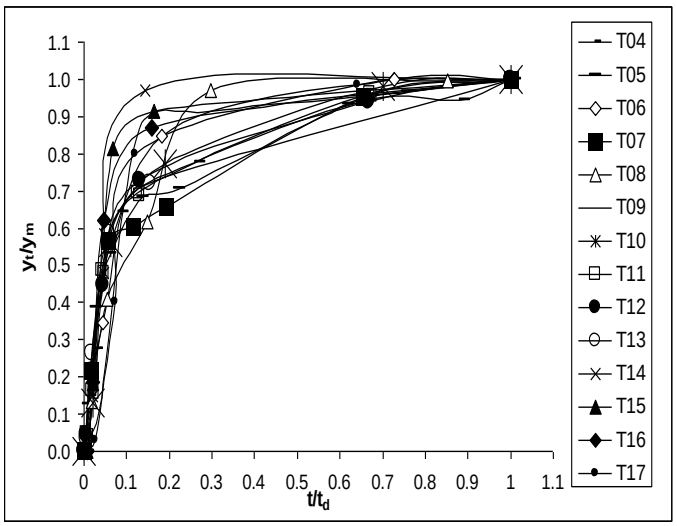


Figure 4. Similarity of scour holes evolution

A second stage is characterized by an increase scour degree much smaller than the first stage. Figure 4 also shows that during this stage, the depth of the scour hole increases globally with a percentage of 25% of the maximum scour hole through a time estimated of 30% of the duration after which the equilibrium stage was reached. As is well known, the increase degree of $y_t/y_m$ depends on the magnitude of the bed-shear stress. Therefore, it can be said that the shear stress acting over the bed reduces with the increase of the scour hole depth.

A final slow stage is that for which the scour achieves equilibrium after a long period of time. The equilibrium phase was assumed to be reached when no transport of sediment particles is observed along the channel. Figure 4 indicates that the bed deformation or the scour hole evolution is extremely slow during this stage. It can be observed that, during a time more than 60% of the duration after which the equilibrium stage was reached, the scour depth increases only with a value around 10% of the maximum scour depth.

### 4.2 *Scour hole shape*

According to the experimental results, it was observed that the scour hole shape depends strongly upon the distance between sills. It was seen that during the first set of tests with an interval length equal to 1m, the scour hole shape is quasi-parabolic. An example (T05) of a three-dimensional scour hole is shown in Figure 5. This configuration is characterized by a scour hole which occupies all of the space between sills. It was also observed that the scour hole dimensions were influenced by the proximity of sills, especially when the flow discharge is elevated.

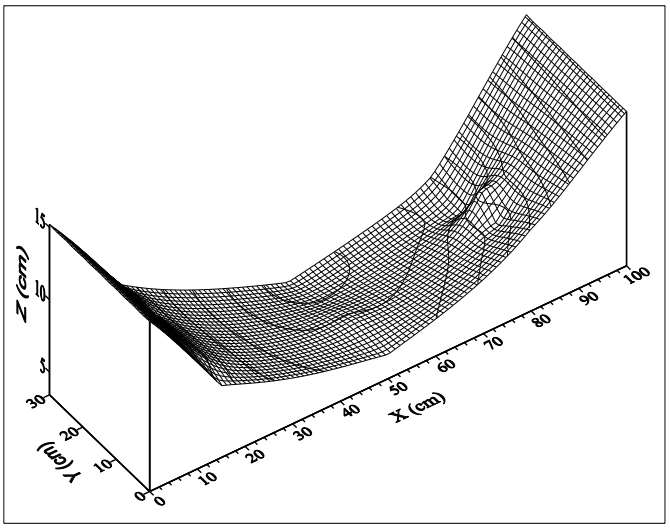


Figure 5. Quasi-parabolic shape

Furthermore, when the interval length between sills is large such as in the cases of the second, the third and fourth sets of tests, which have an interval of 2m, 4m and 3m, respectively, the scour hole shape is similar to a "spoon" profile. An example (T16) of a three-dimensional scour hole profile is shown in Figure 6.

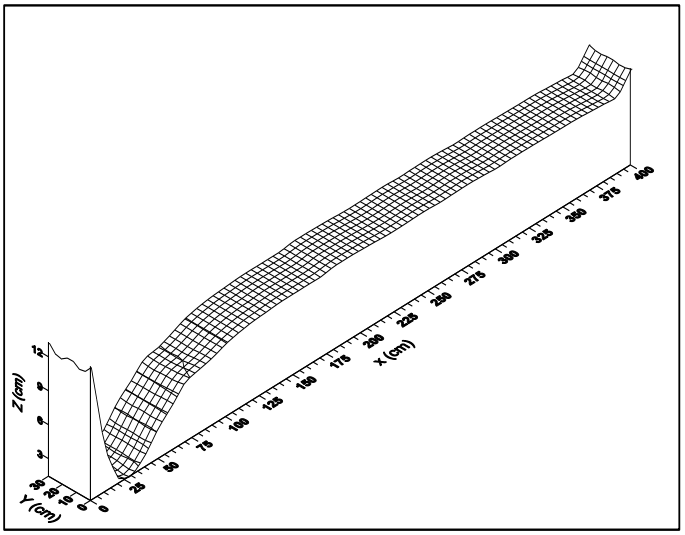

Figure 6. "Spoon" shape

To study the similarity of the scour profile, the values of $y_x/y_m$ at the equilibrium stage have been plotted against $x/l_s$, for T04 to T22, as shown in Figure 7 and Figure 8. $y_x$ and $y_m$ are the depth of the scour hole at the longitudinal distance x (x = 0 m at the upstream sill position) and the maximum scour depth at equilibrium phase, respectively.

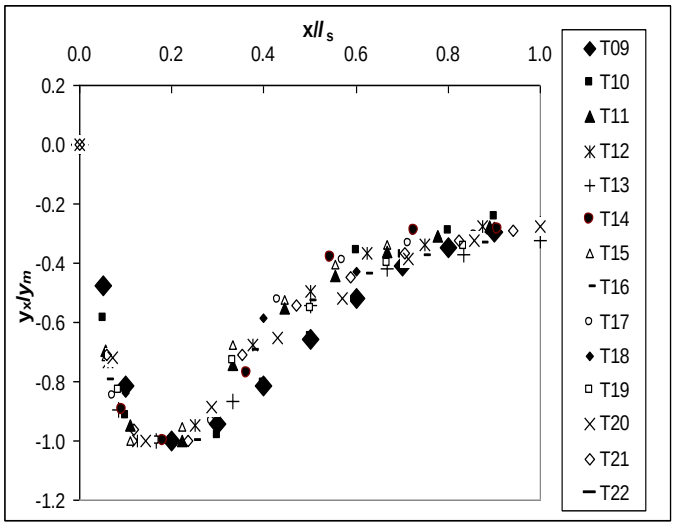

Figure 7. Similarity of the scour profiles

Figure 7 indicates that the scour profiles for T09 to T22 are similar in nature. This result is in agreement with the findings of other authors for other scouring processes (Gaudio et Al., 2000, Chatterjee et Al., 1994). Furthermore, and according to the experimental results, it can be noted that the scour hole profiles for the first set of tests (with a distance between sills of 1m) are not similar in nature, as shown in Figure 8. This is due to the strong influence of the distance between sills for this configuration. Thus, it should be noted that when the length of the scour hole is comparable to the distance between sills, 'the sills interfere' with the development of the scour (Gaudio et Al., 2000).

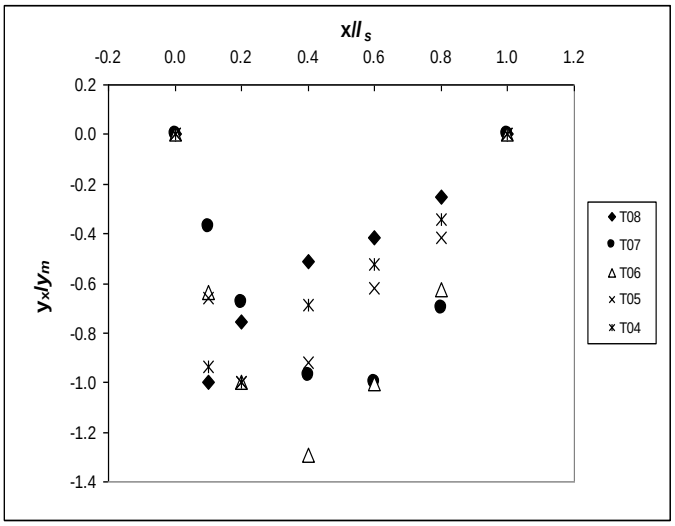

Figure 8. Non-similarity of the scour profiles

### 4.3 *Scour hole dimensions at equilibrium stage*

The non-dimensional parameters for the experimental work discussed here have been determined for each test and illustrated in table 3. Recall that over a sill with a small thickness, the depth of the flowing water fluctuates around the critical flow depth. A comparative study between the flow depth over sills, $h_u$, measured during the experimental work and the critical flow depth, $h_c$, calculated for each test is presented in table 4. It can be seen that the maximum rate of variation between the measured and calculated flow depth (indicated by r %) is 14.77% and the minimum is 0.49%. The average variation for all tests is 7.89%, which is considered very small. Thus, the flow depth over sill can be estimated with the formula of the critical flow depth, $h_c$:

$$h_u \approx h_c = \left(\frac{q^2}{g}\right)^{1/3} \tag{6}$$

According to these simplifying assumptions, equations (5) can be reduced to:

$$\frac{y_m}{h_u} \text{ or } \frac{l_s}{h_u} = f\left(\frac{\Delta LS_0}{h_u}\right) \tag{7}$$

The plot of $y_m/h_u$ versus $\Delta LS_0/h_u$ for the tests of the scour hole which are similar in nature, as shown in Figure 9, indicates that all the points fall approximately on a single line. So, the linear regression of these points leads to the first of equations (7) to become:

$$\frac{y_m}{h_u} = 0.714\frac{\Delta LS_0}{h_u} + 0.989\,. \tag{8}$$

This equation is valid for $0.405 \leq \Delta LS_0/h_u \leq 2.142$, with a correlation coefficient $R^2 = 0.88$.

The plot of $l_s/h_u$ against $\Delta LS_0/h_u$ of the same tests, as shown in Figure 10, leads to the following relationship:

$$\frac{l_s}{h_u} = 4.6083\frac{\Delta LS_0}{h_u} + 31.006 \tag{9}$$

This equation is valid for $0.405 \leq \Delta LS_0/h_u \leq 2.142$, with a correlation coefficient $R^2 = 0.836$.

Table 3. Non-dimensional parameters

| No. | Test | $y_m/hu$ | $q^2/\Delta g h_u^3$ | $\Delta LS_o/h_u$ | $\Delta d_{50}/h_u$ | $l_s/h_u$ |
|---|---|---|---|---|---|---|
| 1 | T04 | 1.142 | 0.676 | 0.417 | 0.087 | (*) |
| 2 | T05 | 1.627 | 0.423 | 0.261 | 0.055 | (*) |
| 3 | T06 | 1.085 | 0.855 | 0.556 | 0.116 | (*) |
| 4 | T07 | 1.701 | 0.403 | 0.230 | 0.048 | (*) |
| 5 | T08 | 1.481 | 0.574 | 0.330 | 0.069 | (*) |
| 6 | T09 | 1.525 | 0.665 | 0.822 | 0.086 | 34.76 |
| 7 | T10 | 1.343 | 0.586 | 0.673 | 0.070 | 32.04 |
| 8 | T11 | 1.295 | 0.423 | 0.523 | 0.055 | 29.50 |
| 9 | T12 | 1.287 | 0.398 | 0.453 | 0.047 | 28.75 |
| 10 | T13 | 1.287 | 0.375 | 0.405 | 0.042 | 28.53 |
| 11 | T14 | 2.386 | 0.722 | 1.773 | 0.093 | 43.72 |
| 12 | T15 | 2.102 | 0.574 | 1.320 | 0.069 | 39.54 |
| 13 | T16 | 2.065 | 0.421 | 1.043 | 0.055 | 38.58 |
| 14 | T17 | 2.453 | 0.850 | 2.142 | 0.112 | 41.51 |
| 15 | T18 | 1.898 | 0.788 | 1.606 | 0.112 | 37.74 |
| 16 | T19 | 1.767 | 0.668 | 1.233 | 0.086 | 34.76 |
| 17 | T20 | 1.663 | 0.597 | 0.997 | 0.070 | 32.79 |
| 18 | T21 | 1.606 | 0.468 | 0.814 | 0.057 | 32.50 |
| 19 | T22 | 1.516 | 0.407 | 0.687 | 0.048 | 31.77 |

(*)Quasi-parabolic shape of the scour hole

Table 4. Values of $h_u$ and $h_c$

| No. | Test | $h_u$ (m) | $h_c$ (m) | r (%) |
|---|---|---|---|---|
| 1 | T04 | 0.034 | 0.035 | 3.69 |
| 2 | T05 | 0.054 | 0.048 | 11.32 |
| 3 | T06 | 0.026 | 0.029 | 12.15 |
| 4 | T07 | 0.062 | 0.054 | 12.69 |
| 5 | T08 | 0.043 | 0.042 | 1.81 |
| 6 | T09 | 0.035 | 0.036 | 3.14 |
| 7 | T10 | 0.042 | 0.042 | 1.10 |
| 8 | T11 | 0.054 | 0.048 | 11.30 |
| 9 | T12 | 0.063 | 0.054 | 13.10 |
| 10 | T13 | 0.070 | 0.060 | 14.77 |
| 11 | T14 | 0.032 | 0.034 | 5.99 |
| 12 | T15 | 0.043 | 0.042 | 1.81 |
| 13 | T16 | 0.054 | 0.048 | 11.42 |
| 14 | T17 | 0.027 | 0.030 | 11.93 |
| 15 | T18 | 0.027 | 0.029 | 9.16 |
| 16 | T19 | 0.035 | 0.036 | 3.29 |
| 17 | T20 | 0.043 | 0.042 | 0.49 |
| 18 | T21 | 0.052 | 0.048 | 8.24 |
| 19 | T22 | 0.062 | 0.054 | 12.45 |
| | average | | | 7.89 |

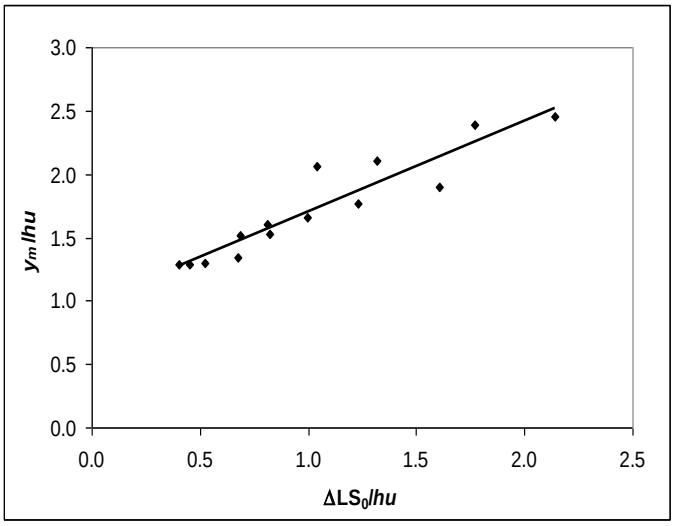


Figure 9. Correlation of the $y_m/h_u$ ratio with $\Delta LS_0/h_u$ ratio

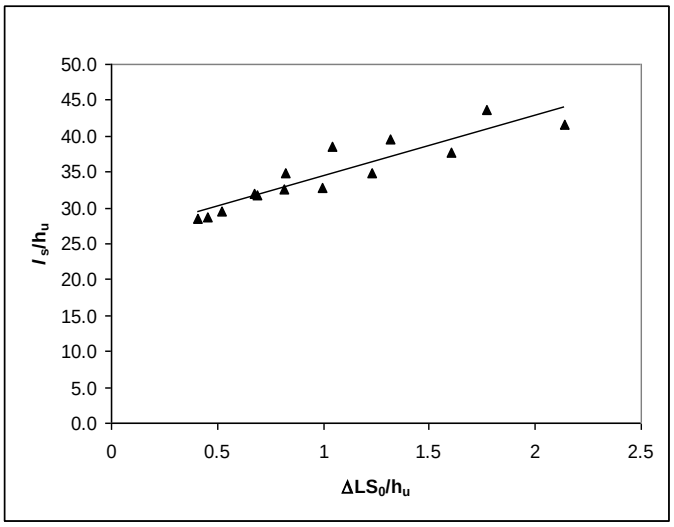


Figure 10. Correlation of the $l_s/h_u$ with $\Delta LS_0/h_u$

## 4.4 *Flow characteristics through the scour hole*

During all the experimental runs, it was observed that, at the equilibrium stage, the sediment particles through the bed scour hole move in a random fashion without leaving it. In order to study the causes of this observation, measurements of the flow velocities along the scour hole were taken. An example (T16) of flow velocity vector field obtained along the centerline of the channel is shown in Figure 11. The velocity vectors are the resulting mean velocities of the vertical and stream-wise velocity components.

This figure indicates that the stream is very turbulent near the scour hole bed; however, it is smoother and more orderly going toward the free-surface flow and downstream of the equilibrium bed hole. In addition, Figure 11 shows that, near the bed of the scour hole, flow rotationality and vortex trends occurred. Near the free surface the flow is assumed mono-directional due to the dominance of the stream-wise velocity.

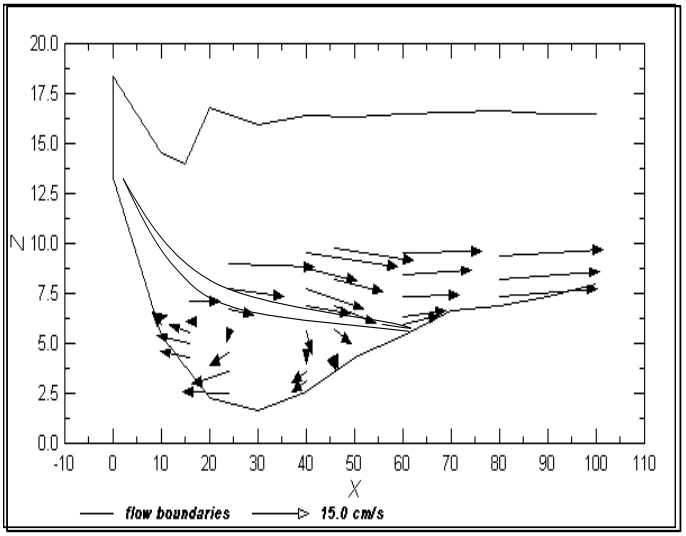

Figure 11. Flow motion along the second scour hole with x in cm and z in cm

### 4.5 *Secondary currents*

It has long been established in academic literature that flow in alluvial rivers is strongly three-dimensional (Peters and Goldberg, 1989). The secondary currents were originally defined by Prandtl (1952) as currents, which occur in the plane normal to the axis of the primary flow. They originate from interactions between the primary flow and gross channel features.

The measurements of the flow velocity along different cross sections of the channel were determined during this experimental work. An example (T13) of the resulting mean velocities of the span-wise and vertical velocities along the transversal centerline of the scour hole is presented in Figure 12. This figure clearly indicates that there is a development of cells of secondary currents through the central cross-section of the scour hole. These secondary currents consisted of two symmetrical cells of helical rotation located near the sidewalls of the channel. The presence of these secondary currents have a direct influence upon the transversal bed profile of the scour hole, resulting in the development of a sand ribbon in its center.

### 4.6 *Turbulence intensity*

The three-components of the flow turbulence index are defined as the ratio of the standard deviation of the stream-wise, span-wise and vertical velocity fluctuation $v_x$', $v_y$', and $v_z$', by the relative flow velocity average $V_x$, $V_y$, $V_z$, respectively. The plot of these components against z/h (z is the distance from the channel bottom and h is the flow depth in the section analyzed), an example (T12) is shown in Figure 13, indicates that the flow turbulence, near the bed of the scour hole, is very intensive, as shown in Figure 13, at z/h = 0.05, the turbulence index of the stream-wise and vertical velocity has a value of 7 and 2.5, respectively, increases extensively to reach the value of 20 and 37 for z/h = 0.15, and decreases gradually to reach the value of 1 and 6 for z/h = 0.4. The results of Figures 12 and 13 explain why the motion of the sediment particles is in a random fashion without leaving the scour hole location at the equilibrium stage.

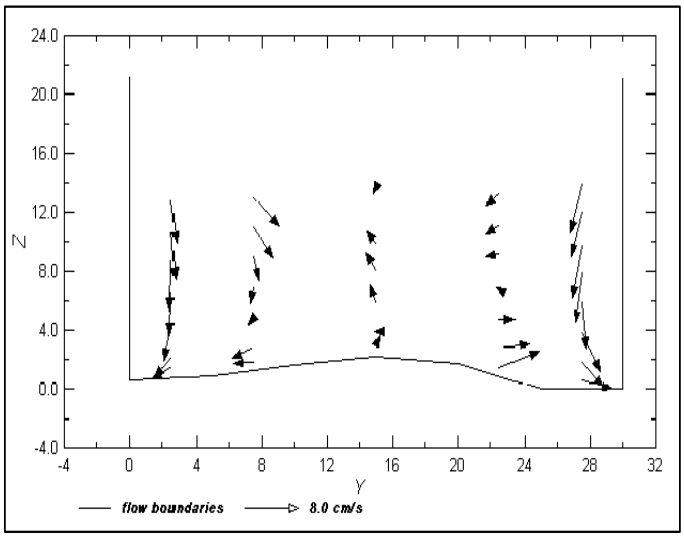

Figure 12. Secondary flow in the cross section at x = 75 cm from the second sill with y in cm and z in cm

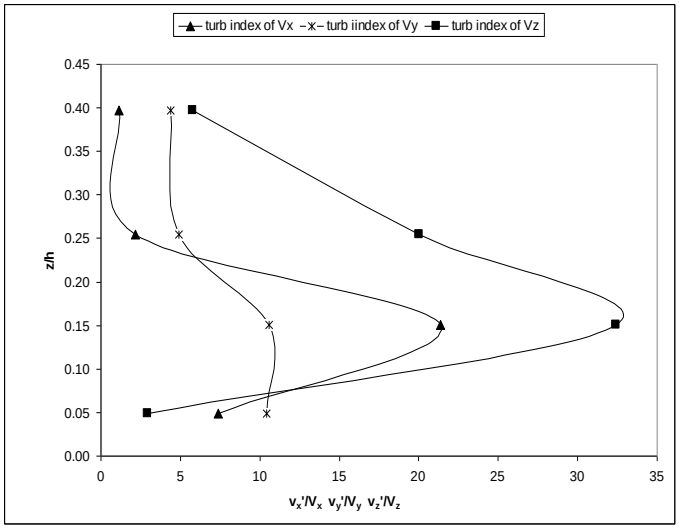

Figure 13. Flow turbulence intensity

## 5. CONCLUSIONS

Four sets of tests were conducted in the hydraulic laboratory of the Mediterranean Agronomic Institute of Bari to predict long term local scour at bed sills. One uniform sediment was used respecting a constant initial bed slop of 0.0086. The experiments show the following results.

The extent of the scour hole is strongly dependent on time. Three stages of the local scour hole development were observed: an initial rapid stage, a progressive stage, and a final decelerated stage.

The scour hole shape depends strongly upon the distance between sills. Two forms of the scour hole

were discovered, i.e. a quasi-parabolic shape occurred with a small distance and a shape similar to a "spoon" profile occurred with large distances. The scour profiles are similar in nature for a large distance between sills, but, not similar for a small distance.

Using classical dimensional analysis, the maximum scour depth and the length of the scour hole at the equilibrium stage were articulated as a function of non-dimensional parameters. According to some logical simplifying assumptions, two empirical formulas (8) and (9) were determined to predict the maximum scour depth, $y_m$, and the length of the scour hole, $l_s$, respectively. The maximum scour depth and the length of the scour hole depend strongly upon the distance between sills.

The bed sills lead to a redistribution of the flow velocity and a flow rotationality. Intensive flow turbulence and vortex trends occurred in addition to secondary currents in the center of the scour hole.

## ACKNOWLEDGEMENTS

The research described and the results presented herein were obtained from an experimental study on long local scouring downstream of bed sills in monogranular sand bed conducted in the hydraulic laboratory of the Mediterranean Agronomic Institute of Bari in 2002.

## REFERENCES

Borman, N.E. 1988. Equilibrium Local Scour Depth Downstream of Grade Control Structures. *Ph.D. Dissertation*. Colorado State University. Fort Collins, CO.

Breusers, H.N.C 1966. Conformity and time scale in two-dimensional local scour; *Proc. Symposium on model and prototype conformity, 1-8.* Hydraulic Research laboratory. Poona (also Delfet hydraulics, Delft, Publication 40).

Chatterjee, S. S. Ghosh, S.N. & Chatterjee, M. 1994. Local scour due to submerged horizontal jet, *Journal of hydraulic engineering ASCE*, 120(8): 973-991.

Gaudio, R. Marion, A. & Bovolin, V. 2000. Morphological effects of bed sills in degrading rivers. *Journal of hydraulic research*, Vol 38. NO2: 89-96.

Habib, E. Mossa, M. & Petrillo, A. 1994. Scour downstream of hydraulic jump. conference papers, *The international journal on hydropower & dams, Modelling, testing & monitoring for hydro.Plants, Budapest*. Hungary: 591-602.

Hoffmans, G. J. C. M. & Krystian, W. Pilarczyk 1995. Local scour downstream of hydraulic structures, *Journal of hydraulic engineerin*, ASCE. 121(4): 326-339.

Hoffmans, G. J. C. M. & Verheij, H. J. 1997, Scour manual. A.A. Balkema, Rotterdam, Brookfield.

Hoffmans, G. J. C. M. 1998. Jet scour in equilibrium phase, *Journal of hydraulic engineering ASCE*. 124(4): 430-437.

Farhoudi, J. & Smith, K. V. H. 1985. Local scour profiles downstream of hydraulic jump. *Journal of hydraulic research*. Vol 23, No 4: 343-358.

Kandasany, J. K. & Melville, B. W. 1998. Maximum scour depth at bridge piers and abutments. *Journal of hydraulic research*. Vol 36, NO 2: 183-197.

Peters, D.D. & Goldberg, A. 1989. Flow data in large alluvial channels. In Maksimovic and Radojkovic (eds). *Computational modeling and experimental methods in hydraulics*. Elsevier, London.

Prandtl, L. 1952. Essentials of fluid dynamics. Blackie. London. 452pp.

Smith, C.D. & Strang, D.K. 1967. Scour in stone bed. Proceedings of the Twelfth Congress of the International Association for Hydraulic Research. *Fort Collins, CO. September 11-14, 1967*. Colorado State University. Vol. 3: 65-73.

Van der Meulen, T. & Vinje, J.J. 1995. Three-dimensional local scour in non-cohesive sediments, *Proc. 16th IAHR-congress*. Sao Paulo. Brasil (also Delft Hydraulics, Delft Publication 180).